Plant Science 302 (2021) 110712

Contents lists available at ScienceDirect

Plant Science

journal homepage: www.elsevier.com/locate/plantsci

Glycyrrhizin, the active compound of the TCM drug *Gan Cao* stimulates actin remodelling and defence in grapevine

Hao Wang *, Michael Riemann, Qiong Liu, Johannes Siegrist, Peter Nick

Molecular Cell Biology, Botanical Institute, Karlsruhe Institute of Technology, Fritz-Haber-Weg 4, D-76131 Karlsruhe, Germany

ARTICLE INFO

Keywords:
Actin
Defence
Glycyrrhizin
Grapevine
Phytoalexins
RboH

ABSTRACT

Actin remodelling by a membrane-associated oxidative process can sense perturbations of membrane integrity and activate defence. In the current work, we show that glycyrrhizin, a muscle relaxant used in Traditional Chinese Medicine, can activate oxidative burst and actin remodelling in tobacco BY-2 cells, which could be suppressed by diphenylene iodonium, an inhibitor of NADPH oxidases. Glycyrrhizin caused a dose-dependent delay of proliferation, and induced cell death, which was suppressed by addition of indole-acetic acid, a natural auxin that can mitigate RboH dependent actin remodelling. To test, whether the actin remodelling induced by glycyrrhizin was followed by activation of defence, several events of basal immunity were probed. We found that glycyrrhizin induced a transient extracellular alkalinisation, indicative of calcium influx. Furthermore, transcripts of phytoalexins genes, were activated in cells of the grapevine *Vitis rupestris*, and this induction was followed by accumulation of the glycosylated stilbene α-piceid. We also observed that glycyrrhizin was able to induce actin bundling in leaves of a transgenic grape, especially in guard cells. We discuss these data in frame of a model, where glycyrrhizin, through stimulation of RboH, can cause actin remodelling, followed by defence responses, such as calcium influx, induction of phytoalexins transcripts, and accumulation of stilbene glycosides.

1. Introduction

Grapevine (*Vitis vinifera*) is among the fruit crops with the highest cash yield per area and has shaped entire cultures, especially in Europe and the Near East [1]. The impact on human culture is linked with the high sugar content and pleasant taste of the fruits, but also makes this crop very attractive for a couple of pathogens. While American wild species of *Vitis* have co-evolved with several important pathogens, the wild ancestor of this crop, the European Wild Grape (*Vitis sylvestris*), had evolved in isolation, and was, therefore, a naïve host, when these pathogens entered Europe in the second half of the 19th century in consequence of economic globalisation. Especially the Downy Mildew of Grapevine (caused by the oomycete *Plasmopara viticola*) has developed into one of the most devastating diseases in viticulture around the world. In order to control this severe pathogen, excessive amounts of fungicides are applied to the vineyards: around 70 % of European fungicide consumption (more than 100 000 t p.a.) goes on account of viticulture [2], which creates a very negative ecological footprint and promotes the spread of fungicide resistance, even in form of multidrug resistance [3]. To reduce fungicide load, web-based prediction systems, such as Vitimeteo, have been successfully implemented [4], but such systems require considerable expertise from the side of the farmers. Also new resistant varieties, harbouring resistance factors from American and Siberian wild grapes [5], have allowed to reduce fungicide load considerably, especially in Germany. However, the consumer acceptance of these new varieties is still not very pronounced. Therefore, alternative strategies are warranted. For instance, boosting the innate immunity of the host would allow to contain pathogens at lower fungicide dosages.

To deal with biotic attacks, plants have evolved a particular two-layer innate immune system. The first layer (designated as MTI for microbial molecular pattern triggered immunity) recognises and responds

Abbreviations: TCM, Traditional Chinese Medicine; PAMP/MAMP, pathogen-/microbe-associated molecular pattern; MTI/PTI, MAMP- /PAMP triggered immune; ETI, effector-triggered immunity; ROS, reactive oxygen species; PAL, phenylalanine ammonia lyase; StSy, stilbene synthase; RS, resveratrol synthase; IAA, indole-3-acetic acid; 2,4-D, 24-dichlorophenoxyacetic acid; BY-2, *Nicotiana tabacum* L. cv Bright Yellow 2; AtFABD2, *Arabidopsis thaliana* fimbrin actin-binding domain 2; DPI, diphenylene iodonium chloride; WT, wild type.

* Corresponding author.
E-mail addresses: hao274143118@gmail.com (H. Wang), michael.riemann@kit.edu (M. Riemann), liuqionglandmail@gmail.com (Q. Liu), johannes.siegrist@gmail.com (J. Siegrist), peter.nick@kit.edu (P. Nick).

https://doi.org/10.1016/j.plantsci.2020.110712
Received 5 April 2020; Received in revised form 28 September 2020; Accepted 3 October 2020
Available online 14 October 2020

to molecules which are common in many classes of microbes (including non-pathogens), while the second layer (termed ETI for effector triggered immunity) responds to specific pathogens by recognition of their effectors, by which such co-evolved pathogens quell the first level of host immunity [6]. Both, MTI and ETI, are associated with complex defence signalling, which includes calcium influx, release of reactive oxygen species, activation of mitogen-activated protein kinase (MPK), plant hormone synthesis and signalling, metabolic changes, excessive transcriptional reprogramming, and the synthesis and accumulation of phytoalexins and other secondary metabolites [7]. While MTI and ETI trigger overlapping transcriptional responses [8,9], the transcriptional response of ETI is typically faster, stronger, and/or more prolonged than gene expression associated with MTI [9–12]. Moreover, ETI is in most cases (albeit not always) culminating in a specific form of programmed cell death, termed hypersensitive reaction. Also the early responses, upstream of gene expression, overlap between these two layers of innate immunity, but differ in their temporal pattern: A comparative study in grapevine cells [13] revealed that activation of reactive oxygen species initiated earlier and reached higher amplitudes in response to a trigger of ETI, while calcium influx was seen to proceed more swiftly in response to a trigger of MTI. Therefore, despite difference in amplitude and timing, MTI and ETI seem to work in concert when establishing plant immunity [6].

Wild American grapes have co-evolved with the important grapevine pathogen Downy Mildew (*P. viticola*) over millions of years. Therefore, they should have had enough time to evolve ETI and consequently are capable of coping with these pathogens. Introgression of genetic factors linked with this ETI into cultivated grapevine has been a success story [5], but is endangered by new pathogen strains that can break this resistance. Therefore, new approaches to boost basal immunity using novel resistance factors from Chinese [14,15] and European [16–18] wild grapes have been launched. For instance, the novel factor *Rpv10* from *Vitis amurensis* is already successfully employed in commercial varieties in Germany [19]

Although more and more defence-related genes have been found, breeding of grapevine is a lengthy process, and the resulting resistance might turn out of limited durability due to pathogen evolution. As alternative to fungicides or resistance breeding one might attempt to render the immune system of grapevine more sensitive against these pathogens, a strategy that has been termed as 'priming of defence' [20–22]. Basal immunity often confers only a residual level of resistance, especially once it has been quelled by pathogen effectors [23]. Treatments that would activate defence response prior to pathogen invasion, should, therefore evade immune suppression [21]. Since basal immunity is controlled by several genes, activation of basal immunity is effective against a broad range of diseases ("horizontal resistance") and, thus, may be more sustainable than single *R* genes based ETI [23]. The reduction in plant fitness caused by priming is relatively minor, because priming is based on an elevated responsiveness to a given elicitor or MTI, but does not express this costly defence response in the absence of an attack [23]. The epigenetic changes induced during priming, are relatively stable, such that plants develop an immunological memory [20].

Since priming seems to be linked with a change of sensitivity, it is most likely reflected in changes of early signalling. These might involve changes in abundance or structure of receptors at the plasma membrane, or modifications of associated components involved in early signalling. In this context, actin filaments are of interest, since they play a role for the perception of membrane integrity [24]. In fact, actin filaments respond swiftly to defence-related elicitors, or to physical perturbation of membrane integrity. Bacterial harpin proteins [25–27], as well as the phytoalexins resveratrol [28] can cause a remodelling of the dynamic meshwork of cortical actin filaments and their subsequent contraction into actin cables. This dynamic subpopulation of actin [27] plays a role for membrane integrity in animal cells [29], plant cells [30], and oomycetes [31]. Some of the molecular components have been identified: A plant-specific Networked (NET) superfamily of actin-binding proteins specifies different membrane compartments to interact with actin [32]. In *Arabidopsis*, Actin Depolymerising Factor 4 regulates the rapid detachment of actin and formation of actin cables after perturbation of membrane integrity [33,34]. This actin remodelling is often followed by programmed cell death [35] as it often occurs during ETI, for instance in response to the bacterial elicitor harpin [27,35].

While actin remodelling is a hallmark of ensuing programmed cell death (for review see [35]), it does not necessarily culminate in cell death. For instance, bundled actin is also a typical feature of cells that have terminated (or failed to initiate) elongation growth [27]. The link between plant defence and remodelling of cortical actin filaments seems to be formed by reactive oxygen species [24,27,36], generated by the membrane-located NADPH oxidase Respiratory burst oxidase Homologue that, upon membrane passage interact with the actin capping protein [37]. The fact that a similar link between ROS and actin is also found in mammalian and fungal cells [35] indicates that the relationship between ROS and actin has a long evolutionary history.

In our previous work, we could show that glycyrrhizin, the active compound of a plant drug used as *gan cao* (*Glycyrrhiza radix*) in Traditional Chinese Medicine (TCM) can induce zoospore burst in the oomycete grapevine pathogen *P. viticola* [31]. This effect was linked with an inhibition of contractile vacuole activity and dependent on a NADPH oxidase and on actin, which would mean that the ROS-actin circuit is also preserved in these oomycetes. Also in mammalian cells, glycyrrhizin can modulate the generation of ROS. For instance, it can soothe inflammation-dependent contraction of smooth muscles, and, thus, relieve asthma or spasmic bronchitis [38]. Also oxidative burst of neutrophils, a potent mediator of tissue inflammation was inhibited by glycyrrhizin *in vitro* (reviewed Asl and Hosseinzadeh [39]).

Since the actin-ROS circuit is conserved from Oomycetes over plants till mammalian cells, and since this circuit can be stimulated by glycyrrhizin, we would expect that glycyrrhizin can be used as a trigger to activate actin-dependent defence response in plant cells as well. This question was the motivation for the current study. Making use of transgenic tobacco and grapevine cells, as well as transgenic grapevine plants expressing a fluorescent actin maker, and spinning disc confocal microscopy, we can show that glycyrrhizin can induce actin remodelling, and that this remodelling requires the activity of the membrane-located NADPH oxidase. The actin response is followed by activation of phytoalexin synthesis genes and accumulation of glycosylated stilbene phytoalexins. The fact that the actin response induced by glycyrrhizin is followed by cell death bears some resemblance with a hypersensitive response. Interestingly, addition of exogenous indole acetic acid (a natural auxin), which can mitigate glycyrrhizin-induced actin remodelling, also can mitigate cell death indicative of a functional link between actin and activation of programmed cell death. Since glycyrrhizin can activate several early events of grapevine defence, it has potential to develop defence-priming strategies.

2. Materials and methods

2.1. Cell lines and plants

Suspension cells of tobacco BY-2 (*Nicotiana tabacum* L. cv Bright Yellow 2, [40]) and the transgenic actin marker strain GF11, expressing a GFP fusion with the *Arabidopsis thaliana* fimbrin actin-binding domain 2 (*GFP-AtFABD2*) in a stable manner [41] were cultivated as described in Huang et al. [42].

Cell suspension cultures of the grapevine *Vitis rupestris* originating from leaves [43] were cultured as described in Qiao et al. [25] in liquid MS medium on an orbital shaker (KS250 basic, IKA Labortechnik, Germany) at 150 rpm, 25 °C, in the dark at weekly subcultivation intervals.

Transgenic grapevine plants (*Vitis vinifera* cv. Chardonnay, line 10a), expressing the *GFP-AtFABD2* marker [44] were grown in the greenhouse of Botanical Garden, Karlsruhe Institute of Technology (KIT). Fully expanded leaves were excised and used for leaf-disc experiments. From

the same transgenic genotype, suspension cells were established from leaf mesophyll. In short, leaves were surface sterilised with 1% NaOCl for 2 min, and subsequently washed with several cycles of sterile water and 70 % EtOH. After cutting the leaf into 5-mm pieces under sterile conditions, the tissue was then placed on agar with 2.3 g·L^{-1} MS medium basal salts, modification 1 (Duchefa) solidified with 0.5 % (w/v) Gelrite (Roth, Karlsruhe). Media were complemented with 2 g/l sucrose and 1 mg L^{-1} 2,4-D. After 4–6 weeks at 23 °C, the calli were excised and transferred to liquid medium, to generate later suspension cultures. Chardonnay GFP-AtFABD2 cells were cultured as described for *V. rupestris* suspension cells, but supplemented with 50 mg L^{-1} Kanamycin to maintain selective stringency.

2.2. Chemicals

The bacterial elicitor harpin from *Erwinia amylovora* (Pflanzenhilfsmittel, ProAct, Starnberg, Germany; 1% active ingredient Harpin protein) was dissolved in water to yield a stock solution of 300 mg ml^{-1}. An aqueous stock solution of glycyrrhizin (Roth, Karlsruhe, Germany) was prepared to 4 mM. Diphenylene iodonium chloride (DPI; Cayman, United States), a specific inhibitor of NADPH oxidases, was prepared in dimethyl sulfoxide (DMSO) to give a stock solution of 200 μM. Indole-3-acetic acid (IAA; Roth, Karlsruhe, Germany) was dissolved in 96 % ethanol to a stock solution of 5 mM and kept at −20 °C protected from light. Evans Blue (Sigma-Aldrich, Steinheim, Germany) was prepared as a solution of 2.5 % (w/v) in sterilised water and used for viability staining.

2.3. Detection of actin filaments in suspension cells and leaf discs

To test the cellular actin response to glycyrrhizin treatment, 20 μM of glycyrrhizin were used in case of tobacco BY-2 GF11 cells, and 20 or 50 μM glycyrrhizin for the grapevine Chardonnay cells expressing *GFP-AtFABD2* marker. To test the effect of superoxide to the response of actin, we pre-treated the GF11 cells with 200 nM DPI or the equivalent volume of DMSO as solvent control for 30 min before adding 20 μM glycyrrhizin.

To visualise actin in leaf cells, disc of 5 mm diameter were excised from leaves of *V. vinifera* cv. Chardonnay plants expressing the *GFP-AtFABD2* marker using a cork borer. The leaf discs were placed on wet filter paper in Petri dishes and then infiltrated in perfluorodecalin (PFD, Sigma-Aldrich, Steinheim, Germany) for 5 min to increase the specimen transparency. Then, the leaf discs were either treated with water as solvent control, or with 2 mM, or 4 mM glycyrrhizin, respectively.

The cellular details of individual cells or leaf discs were examined under a spinning-disc device (YOKOGAWA CSU-X1 5000) by optical sectioning. The 488 nm emission line of an Ar-Kr laser (Zeiss) was used to excite GFP. Confocal images were recorded with an AxioObserver Z1 (Zeiss, Jena, Germany) equipped with a cooled digital CCD camera (AxioCam MRm) using a 63 x LCI-NeofluarImmCorr DIC objective (NA 1.3) and a spinning-disc device (YOKOGAWA CSU-X 15000). At different time points after onset of the treatments, z-stacks were captured and processed using the Zen 2012 (Blue edition) software platform to generate orthogonal projections from the recorded stacks.

2.4. Quantification of actin reorganisation in GF11 suspension cells

In response to glycyrrhizin, the actin filaments contracted towards the cell centre around the nucleus. To quantify this central contraction of actin filaments, we used the software ImageJ (NIH, Bethesda, United States, https://imagej.nih.gov/ij/) to record fluorescent density profiles over the orthogonal projections, which had been obtained from the confocal z-stacks. We had observed, during preparatory experiments, that the response in the periphery was slower than in the cell centre (Suppl. Fig. S1). To average over the entire cell, we, therefore, used two probing lines parallel to the long cell axis, and then determined the geometrical average by multiplying the two values (since these values are ratios, the use of arithmetic means is not appropriate).

The width of probing lines was chosen as 4 pixels to integrate over small random fluctuations of intensity and thus smoothen the profiles.

The density profiles were exported to a pre-structured Excel sheet (Excel 2013, Microsoft Office, United States) such that the length of the profile was divided into three equal parts, and the intensity over each of these parts was integrated, such that the proportion of the entire signal collected along the probing line falling into the respectively third was automatically calculated. If the actin filaments were evenly distributed, this integral should be the same in all three thirds, if the actin filaments were contracted upon the cell centre, the integral in the central domain should be higher than in the two peripheral thirds. To normalise the values, the integral for the central part was divided by a third of the total integral. A value of 1 would then mean that actin is distributed evenly, a value larger than 1 would mean a contraction of actin to the centre, and a value below 1 means that actin is predominantly concentrated in the periphery and depleted from the centre. During preparatory studies, we had compared the readout for central contraction for those obtained for peripheral depletion (Suppl. Fig. S2). The results were almost identical.

2.5. Quantification of actin filament reorganisation in leaf discs

Since the epidermal cells were considerably smaller and the resolution of actin recorded in leaf discs not sufficient for the above-mentioned quantification strategy, we had to use a different approach, making use of the skew of the intensity histogram as a readout for the distribution of actin filaments in leaf discs. The transition of a fluorescent structure from a symmetrical distribution into bundles or agglomerations should increase the areas with very low pixel values, while the saturation of fluorescent pixels would lead to an underrepresentation of the high values. As a consequence, the intensity histogram will become skewed to the left. While such changes of skew have been used to infer the degree of actin bundling [45,46], it will also increase in case of actin contraction towards the nucleus. We determined this change of skew in time-lapse series of leaf discs to quantify the actin condensation based on the intensity histogram collected over the ROI of orthogonal projections obtained from confocal z-stacks (ImageJ, NIH, Bethesda, United States). For the abaxial side, this was done separately for pavement cells and guard cells. The histogram data were then imported into a pre-structured calculation sheet of Excel 2013 (Microsoft Office, United States) and analysed using the "skew" command. To compensate for the natural variation of initial skew values between leaf discs, we defined as value of actin reorganisation A_r the change of the skew compared to the first measured time point (5 min after adding glycyrrhizin) and normalized for the skew value of this first point: $A_r = \triangle S/S_{t= 5\ min}$.

2.6. Quantification of cell cycle duration

To quantify cell cycle duration, 0.5 mL aliquots of cell suspension were collected daily from days 0 to 4 after adding different concentrations of glycyrrhizin (2, 20, 50 or 100 μM). The cell number per millilitre was determined using a Fuchs-Rosenthal hematocytometer (Thoma Glasbläser, Freiburg) under a light microscope (Zeiss-Axioskop 2 FS, DIC illumination, ×20 objective). Doubling times were estimated from these cell density values as described in [42] based on 1500 individual cells per data point.

2.7. Quantification of cell mortality

To quantify cell mortality, the Evans Blue dye exclusion test (Gaff and Okong'O-Ogola, [47] was used. The dye cannot pass the plasma membrane and therefore will not stain viable cells, while cells that have lost their membrane integrity are stained intensely. Aliquots of cell suspension (0.5 mL) were collected from day 2 after adding different concentrations of glycyrrhizin (50, 100 or 150 μM) alone or combined

with 2 μM IAA, respectively. Each sample was transferred into custom-made chambers to remove the medium, and then the cells were incubated in 2.5 % (w/v) Evans Blue for 3 min. Unbound dye was removed by washing thrice with fresh medium. The frequency of the dead cells (stained in blue) was scored under under a light microscope (Zeiss-Axioskop 2 FS, DIC illumination, ×20 objective). The values reported are based on the observation of 1500 cells from three independent experiments.

2.8. Measurement of extracellular alkalinisation

Extracellular alkalinisation can be used as a rapid readout for the activation of plant immunity, because it reports the co-import of proton with calcium as an earliest known event of signalling [48]. Extracellular alkalinisation was measured by pH meter (pH 12, Schott Handylab) with a pH electrode (LoT 403-M8-S7/120, Mettler Toledo) after pre-equilibrating *V. rupestris* cells on an orbital shaker for around 60 min and then treated with different concentrations of glycyrrhizin (50 or 100 μM). Values for $\triangle$pH were calculated as differentials of treatment *versus* mock control. Peak values were used as estimate for $\triangle pH_{max}$ and were reached at around 300−900 s (5−15 min).

2.9. RNA extraction, cDNA synthesis and quantitative Real-Time RT-PCR

Total RNA was isolated using the Universal RNA Purification Kit (Roboklon, Berlin, Germany) according to the protocol of the manufacturer. The extracted RNA was treated with an RNase-free DNase (Qiagen, Hilden, Germany) to remove any potential contamination by genomic DNA. The mRNA was transcribed into cDNA using the M-MuLV cDNA Synthesis Kit (New England Biolabs, Frankfurt am Main, Germany) according to the instructions of the manufacturer. To prevent RNA degradation, RNase inhibitor (New England Biolabs, Frankfurt am Main, Germany) was added. The amount of RNA template was adjusted to 1 μg.

To test, whether glycyrrhizin elicited the expression of defence-related genes (in this study we measured steady-state transcript levels for phenylalanine ammonia lyase, PAL, stilbene synthase, StSy, and resveratrol synthase, RS as markers), *Vitis rupestris* cells were treated with 50 μM, 100 μM glycyrrhizin, or with water (solvent control) for 0, 1, 3, 5 hours. The abundance of transcripts was evaluated by quantitative Real-Time RT-PCR using the primers listed in Table S1 of the supplementary material. The Real-Time RT-PCR was performed in a Bio-Rad CFX detection system (CFX96 Touch™ Real-Time PCR Detection System, Bio-Rad, California, United States) according to the instructions of the manufacturer with the following programs: initial strand separation at 95 °C for 3 min followed by 39 cycles of strand separation at 95 °C for 15 s; annealing and elongation at 60 °C for 40 s. Values for relative transcript abundance were calculated using elongation factor 1α and actin as internal standards [49]. The recorded C_t values were then used to estimate the steady-state level of the respective transcript using the $2^{-\Delta\Delta Ct}$ method [50].

2.10. Quantification of stilbene biosynthesis

To test, whether the transcript of stilbene synthase (*StSy*) was accompanied by the final product generated by this enzyme, *V. rupestris* cells were treated either with 100 μM glycyrrhizin, or with 9 $\mu g \cdot ml^{-1}$ Harpin as a positive control for 10 h. Water was used as negative control. Cells were drained from culture medium by a vacuum of 800 pa (Vacuubrand CVC2, Brand, Germany), frozen in liquid nitrogen, and then stored at −80 °C until future analysis. Aliquots of 3 g fresh weight of untreated control or treated cells were homogenised with 20 ml of 80 % (v/v) methanol in water by an ultrasonic processor (UP100H, Hielscher, Germany) for 3 min. The homogenate was incubated for 2 h in the dark at room temperature in a rotatory shaker and filtered through a filter paper (Whatman® Grade 1, Schleicher & Schüll, Germany). The filtrate was concentrated to a residual volume 5 ml in a glass tube at 40 °C (Heating Bath B490, BÜCHI, Germany) at 280 rpm (Rotavapor R-205, BÜCHI, Germany), under a vacuum of 100 Pa (Vacuubrand CVC2, Brand, Germany). Stilbenes were extracted from the aqueous phase by adding 2 ml 5% (w/v) $NaHCO_3$, and three aliquots of 5 ml ethyl acetate. The pooled ethyl acetate phase was completely dried, and the residue suspended in 2 ml of methanol before being injected into the HPLC.

Analysis of stilbenes was carried out on a high-performance liquid chromatograph, HPLC (Agilent, 1200 series, Waldbronn, Germany) as described in Chang et al. (2011). *Trans*-resveratrol, *trans*-piceid, and δ-viniferin were quantified using external standards based on retention time and UV-VIS spectra. The standards for *trans*-resveratrol (Sigma-Aldrich, Steinheim, Germany), *trans*-piceid (Phytolab, Vestenbergsgreuth, Germany), and δ-viniferin (Sigma-Aldrich, Steinheim, Germany) were dissolved in methanol to a concentration of 100 mg l^{-1}. Calibration curves for quantification of the samples were determined using these standards and found to be linear (r^2>0.99). At least three independent experimental series were conducted.

2.11. Statistical analyses

All data represent the mean from at least three independent experimental series. Bars are standard errors. Statistical significance was assessed using Microsoft Office Excel Software (version 2013) and using a student *t*-test with defining *as $P \leq 0.05$, and as **$P \leq 0.01$.

3. Results

In the current work, we followed the cellular responses to glycyrrhizin with a focus on actin and defence. For quantitative phenotyping of these responses, we used a tobacco BY-2 strain expressing the actin-binding domain 2 of *Arabidopsis thaliana* fimbrin (*AtFABD2*) infusion with GFP, because this cell strain with its pronounced axiality of division and expansion allows to phenotype actin-dependent morphological responses in a reliable manner [42]. To probe for defence responses including phytoalexins synthesis, we were then changing to suspension cells and plants of the economically relevant variety *V. vinifera* cv. Chardonnay expressing the same fluorescent actin marker.

3.1. Glycyrrhizin can induce actin remodelling in tobacco BY-2 cells, which is blocked by Diphenylene Iodonium

To test whether glycyrrhizin could elicit an actin response in plant cells, we used this compound to treat suspension cells of the tobacco actin marker line GF11 [41]. As shown in Fig. 1B, a treatment with 20 μM glycyrrhizin induced a clear response of actin filaments which was evident as early as 10 min after addition of the compound and not seen in the solvent (water) control (Fig. 1A). This actin response included bundling of actin strands and a contraction towards the nucleus. To validate this actin condensation statistically, we quantified the central contraction of actin filaments by quantitative image analysis (Fig. 2A). While in the negative control no significant change of actin organisation was seen over the entire time of the experiment (60 min), glycyrrhizin induced a strong increase of central contraction which became significant from 15 min after addition of the compound (Fig. 2B, left).

To test, whether this actin response to glycyrrhizin was dependent on an apoplastic oxidative burst by the membrane-located NADPH oxidase, we pre-treated the cells for 30 min with 200 nM of the specific inhibitor diphenylene iodonium (DPI), or the same volume DMSO as solvent control for DPI, before adding 20 μM glycyrrhizin (Fig. 2B, right). While DPI alone did not cause any significant actin response, it was able to efficiently suppress the actin contraction caused by glycyrrhizin almost down to the level as seen in the negative control. Also, in the solvent control (0.1 % v/v DMSO), no actin response was observed (data not shown).

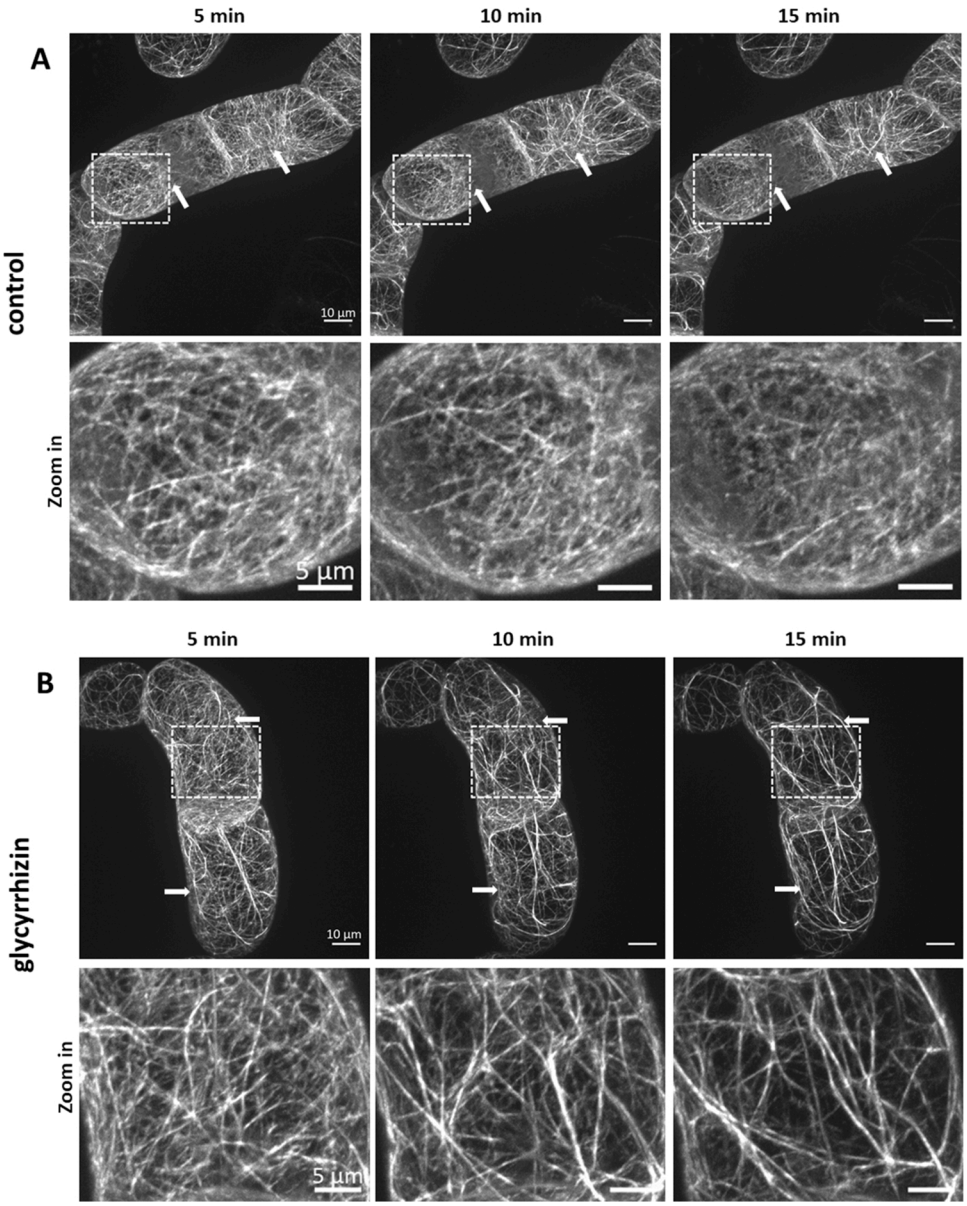

Fig. 1. Response of actin filaments to glycyrrhizin in non-cycling tobacco BY-2 cells expressing the actin marker fimbrin actin-binding domain 2 in fusion with GFP. **A** control cells treated with water, **B** cells treated with 20 µM of glycyrrhizin. Geometric projections of confocal z-stacks are shown as an overview (upper row) and zoomed in to show the details of actin remodelling (lower row). Cells were treated in the expansion phase of the culture following proliferation. The location of nucleus is shown with white arrows.

3.2. Glycyrrhizin shifts tobacco BY-2 cells from proliferation to cell death dependent on actin

Actin bundling and contraction is often a hallmark heralding programmed cell death. We, therefore, quantified the effect of glycyrrhizin on the length of the cell cycle and the viability of the treated cells. In order to find out, whether the cellular effects produced by glycyrrhizin depend on actin, we compared non-transformed wild-type cells with the GF11 cells, since overexpression of the *AtFABD2* marker is known to cause a mild reduction of actin dynamics [42]. When we followed the response of doubling time during the proliferative phase of the culture over different concentrations of glycyrrhizin in the wild type (Fig. 3A), we found an apparent increase of doubling time from less than a day in non-treated cells to more than 4 days in the presence of 100 µM of glycyrrhizin. This delay in cycling was significant from 50 µM glycyrrhizin, but not seen at lower concentrations. In the line overexpressing the fimbrin actin binding domain 2 marker, this increase of doubling time was reduced (Fig. 3B). Here, treatment with 100 µM delayed the cycling to only 2 days, and at 50 µM, no significant delay was seen, contrasting with the situation in the non-transformed wild type. It should be noted that 20 µM of glycyrrhizin, a concentration that had caused actin contraction (Fig. 2B, left), did not delay the cycling of neither the WT, nor that of the transgenic line.

To find out, whether the prolongation of cell cycle duration is associated with actin-dependent cell death, we scored mortality after two days of glycyrrhizin treatment using the Evans Blue dye exclusion test. In the non-transformed wild type (Fig. 3C), mortality was sharply increased to almost 40 % already at a concentration of 50 µM of glycyrrhizin. By doubling this concentration to 100 µM, this value hardly changed, while for 150 µM mortality could be driven to around 50 %. In GF11 (Fig. 3D), higher concentrations of glycyrrhizin were needed to obtain the same level of mortality as in the wild type. Here, 50 µM were still not saturating, producing mortality of around 15 %, while a doubling of this concentration to 100 µM produced 40 %, a value that could not be significantly driven further by raising the concentration of glycyrrhizin to 150 µM. In other words: the GF11 line, where actin filaments are mildly stabilised, is less sensitive to glycyrrhizin induced cell death indicative of a role for actin in this cellular response. To test this assumption, we repeated the experiment in the presence of low concentrations of the natural auxin indole acetic acid (2 µM IAA), which can

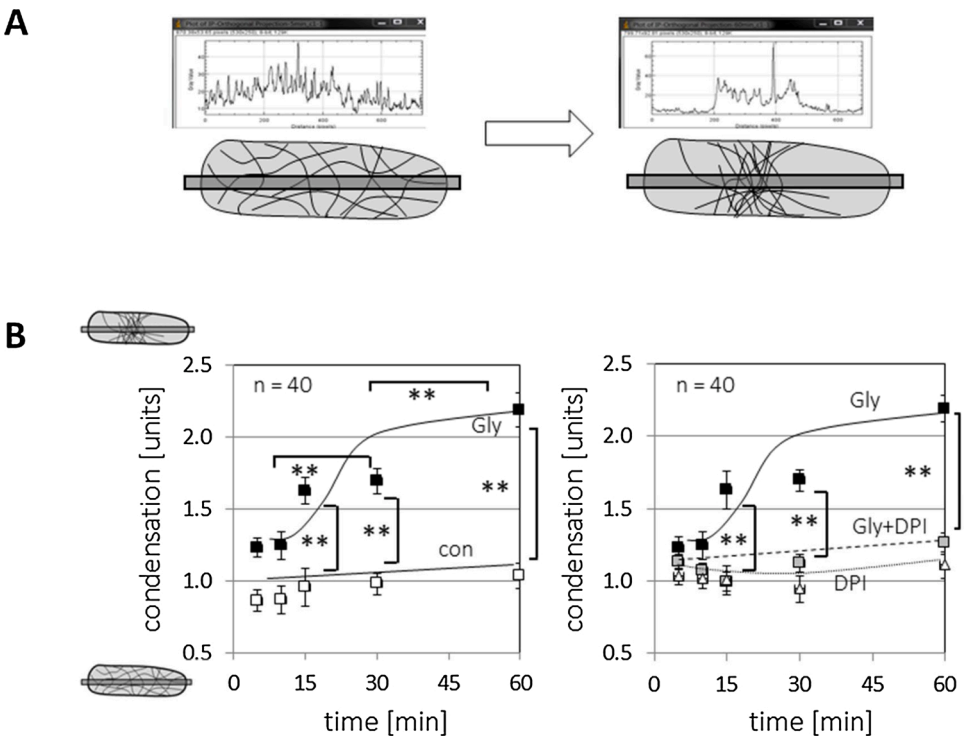

Fig. 2. Quantification of the actin condensation response to glycyrrhizin in non-cycling tobacco BY-2 cells expressing the actin marker fimbrin actin-binding domain 2 in fusion with GFP. **A** Schematic depiction of the strategy to quantify the actin response by measuring a profile of fluorescence intensity along a probing line. **B** Time course of actin condensation determined from time-lapse series. Left: response to 20 μM of glycyrrhizin compared to the solvent control (water), right: effect of pre-treatment with 200 nM of diphenylene iodonium (DPI) 30 min before addition of 20 μM glycyrrhizin as compared to same concentration of glycyrrhizin alone or DPI alone. Data represent mean values and standard errors from 40 individual time series collected from at least three independent biological experiments. Statistical significance was assessed using a student *t*-test with defining *as $P \leq 0.05$, and as **$P \leq 0.01$.

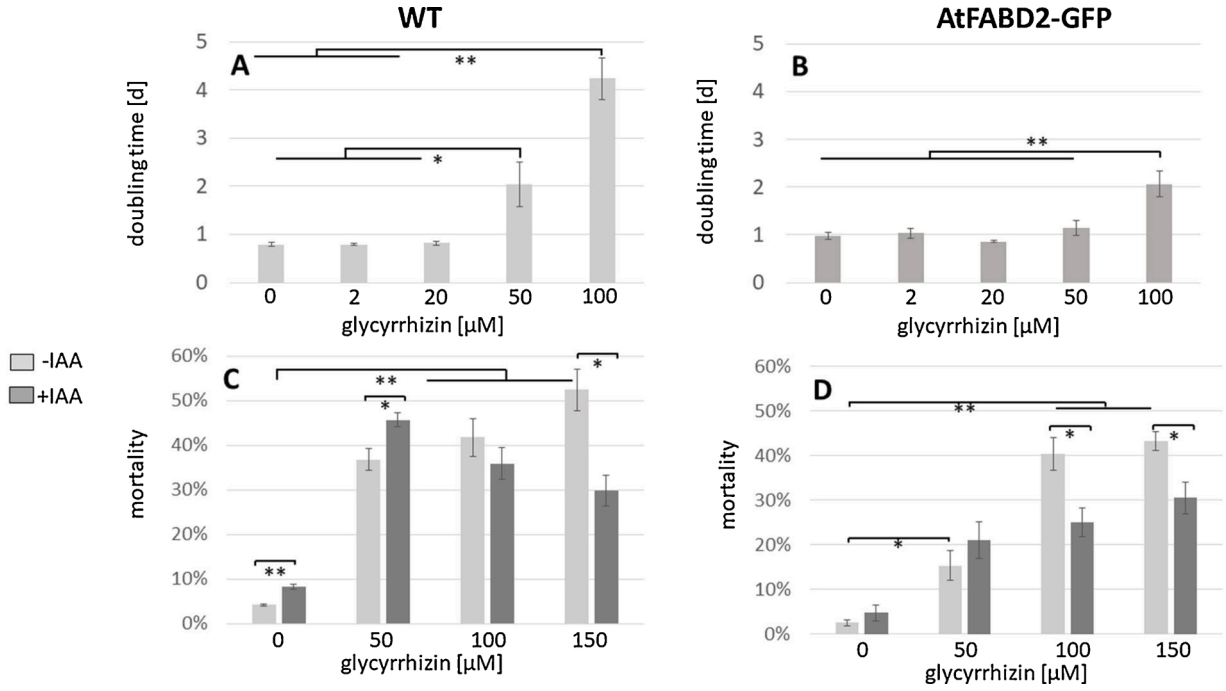

Fig. 3. Dose-response relations over glycyrrhizin for doubling time (**A, B**) and mortality (**C, D**) in non-transformed tobacco BY-2 cells (WT, **A, C**), and cells expressing the actin marker *Arabidopsis thaliana* fimbrin actin-binding domain 2 in fusion with GFP (AtFABD2-GFP, **B, D**). Mortality was assessed either with glycyrrhizin alone (light grey bars) or in combination with 2 μM of indole-acetic acid (IAA, dark grey bars) at day 2 after subcultivation and addition of the compounds. Data represent mean values and standard errors from 1500 cells per data point and experiment and at least three independent biological experiments. Statistical significance was assessed using a student *t*-test with defining *as $P \leq 0.05$, and as **$P \leq 0.01$.

inhibit actin bundling [24,42,51]. We observed that IAA reduced glycyrrhizin-induced mortality, but only for the higher concentrations of glycyrrhizin, and only partially (Fig. 3C, D, dark grey bars). For the non-transformed BY-2 cells (Fig. 3C), a significant effect was only seen for 150 μM of glycyrrhizin (here, auxin decreased mortality from around 50% to 30%). For the line overexpressing the actin marker (Fig. 3D), the auxin effect was manifest already at 100 μM of glycyrrhizin. Thus, auxin, as suppressor of actin bundling, can mitigate the effect of glycyrrhizin, and this mitigation is different when actin filaments are stabilised by overexpression of the *AtFABD2* marker, which both supports a role of

actin filaments for glycyrrhizin-induced cell death.

3.3. Glycyrrhizin can induce apoplastic alkalinisation in grapevine cells

Alkalinisation of the apoplast is one of the earliest responses of plants cell to microbial elicitors [48]. We, therefore, used extracellular alkalinisation to monitor a potential activation of defence responses by glycyrrhizin in suspension cells of the wild grape *Vitis rupestris*, since these cells produce a robust and stable defence response to elicitation [25]. When glycyrrhizin was added to the cell suspension, the pH increased rapidly and without any lag phase culminating a few 10 min. after addition of the compound to decrease again at a slower pace (Fig. 4A). Both, the velocity and the amplitude of this response were dependent on the dose of glycyrrhizin: For 100 µM of glycyrrhizin the peak was reached faster (in about 5 min) compared with 50 µM, where the peak was observed later, at about 10 min. Likewise, for 100 µM of glycyrrhizin the alkalinisation reached almost 0.5 pH units, while for 50 µM only half of this value (0.25 units) were seen (Fig. 4B). The dose dependent, transient activation of a transient extracellular alkalinisation indicates that glycyrrhizin can specifically activate a calcium influx channel.

3.4. Glycyrrhizin can induce expression of phytoalexin genes in grapevine cells

As glycyrrhizin can elicit an apoplastic alkalinisation indicative of an activation of defence, we wondered, whether this early response would be followed by induction of defence-related transcripts, especially of those relevant for phytoalexin synthesis. We selected phenylalanine ammonium lyase (*PAL*) as the first committed step of the phenylpropanoid pathway, and resveratrol synthase (*RS*) and stilbene synthase (*StSy*) representing the first committed step of the stilbenoid branch. We observed a clear, rapid (from 1 h after addition of the compound) and stable induction of *PAL* and *RS* transcripts for 100 µM glycyrrhizin (Fig. 5), while 50 µM induced only a transient response that decline after peaking at 1 h. The pattern for *StSy* differed – here, the induction was much slower (requiring 3 h to become significant) and weaker (only half of the induction seen in *RS*). Again, the response induced by 50 µM did not increase over time but rested at the level reached at 3 h.

3.5. Glycyrrhizin can induce accumulation of glycosylated stilbenes

To test whether the accumulation of *RS* and *StSy* transcripts would be followed by accumulation of the respective metabolites (stilbenes), we probed for *trans*-resveratrol as a direct product of resveratrol /stilbene synthase, its glucoside *trans*-piceid, and its oxidative dimer δ-viniferin in response to treatment with 100 µM glycyrrhizin. Suspension cells of *V. rupestris* accumulate mainly stilbene aglycons, such as *trans*-resveratrol and δ-viniferin, but only low levels of the glycosylated stilbenes, such as *trans*-piceid, when they are treated with the bacterial elicitor harpin [13]. To probe for the activity of stilbene synthases, we measured *trans*-resveratrol, its glucoside *trans*-piceid, and its oxidative dimer δ-viniferin by HPLC in *V. rupestris*, after 10 h incubation with either water as solvent control, with 100 µM glycyrrhizin, or with 9 $\mu g \cdot ml^{-1}$ harpin as positive control, respectively (Fig. 6). We observed that the steady-state level of *trans*-resveratrol was increased around 6-fold in response to glycyrrhizin, as compared to the solvent control, while the glycosylated derivative of *trans*-resveratrol, *trans*-piceid was elevated around 2.5-fold over the value seen in the solvent control, and the oxidative dimer δ-viniferin was elevated over the solvent control by a factor of around two. This pattern indicates that trans-resveratrol is formed to a certain extent, but then glycosylated preferentially, while only a small proportion is converted into the non-glycosylated viniferins. This pattern is in stark contrast to the response of the same cells to harpin, which was used as positive control for the ability of these cells to produce a stilbene response. Here, trans-resveratrol accumulated around 40-fold over the solvent control, and δ-viniferin even around 100-fold over the solvent control. In contrast, the accumulation of *trans*-piceid was comparable (around 3-fold) as that induced by glycyrrhizin. These data show that glycyrrhizin can induce a significant (but moderate) accumulation of stilbenes, preferentially in glycosylated form, while harpin can induce a strong accumulation of stilbenes, which preferentially are channelled into the non-glycosylated viniferins.

To assess, whether this accumulation of α-piceid would be accompanied by cell death, we scored the mortality of the same cell strain after 48 h. While in the control, mortality was low (below 10 %), the score was strongly induced by 100 µM glycyrrhizin to around 40 %, i.e. to a level very similar to those seen in tobacco BY-2 (Fig. 3C).

3.6. Glycyrrhizin can induce actin remodelling in both, grapevine suspension cells and leaf discs

To test, whether glycyrrhizin can also induce actin remodelling in grapevine, we had expressed the same actin marker (fimbrin actin-binding domain 2 in fusion with GFP) in the commercially relevant grapevine variety *V. vinifera* cv. Chardonnay, from which a suspension cell culture was generated. In the negative control (treated with water as solvent), actin filaments, while progressively bundling over the time on

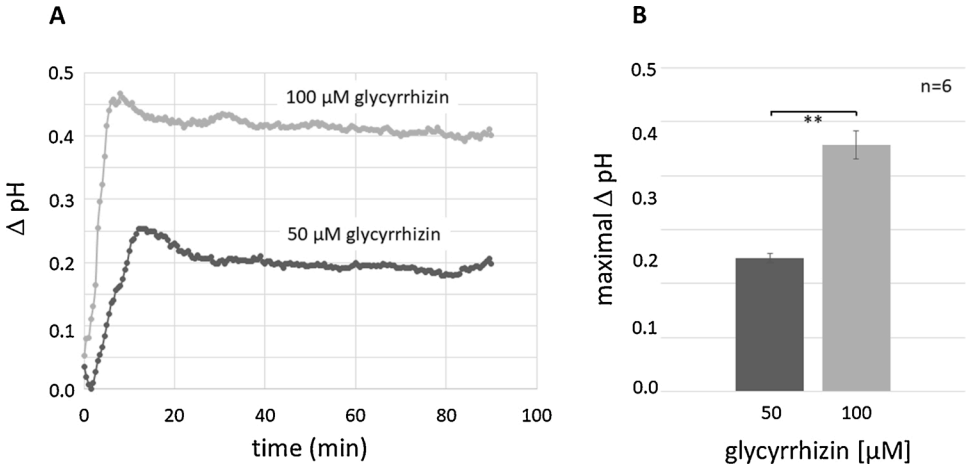

Fig. 4. Glycyrrhizin can induce apoplastic alkalinisation in suspension cells of *Vitis rupestris*. **A** representative time courses of the change in extracellular pH after addition of 50 µM and 100 µM glycyrrhizin. **B** dose dependent increase of maximal pH changes. Data represent mean values, and standard errors from 6 independent biological replications Statistical significance was assessed using a student *t*-test with defining *as $P \leq 0.05$, and as **$P \leq 0.01$.

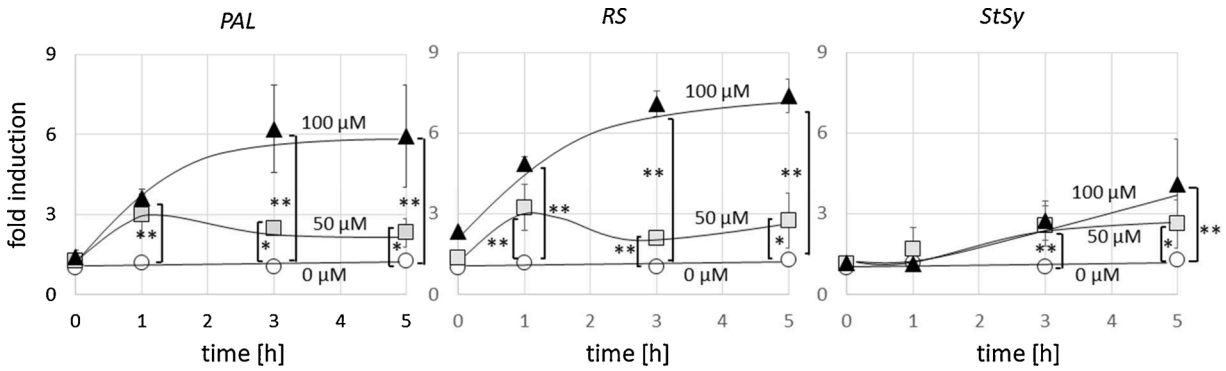

Fig. 5. Glycyrrhizin can induce expression of phytoalexins genes in suspension cells of *Vitis rupestris*. Time course of steady-state transcript levels for phenylalanine ammonium lyase (*PAL*), resveratrol synthase (*RS*), and stilbene synthase (*StSy*) in response to 0 µM (white circles), 50 µM (grey squares), and 100 µM (black triangles) glycyrrhizin. Data represent mean values and standard errors from at least three independent biological replicates conducted in three technical replicates. Statistical significance was assessed using a student *t*-test with defining *as $P \leq 0.05$, and as **$P \leq 0.01$.

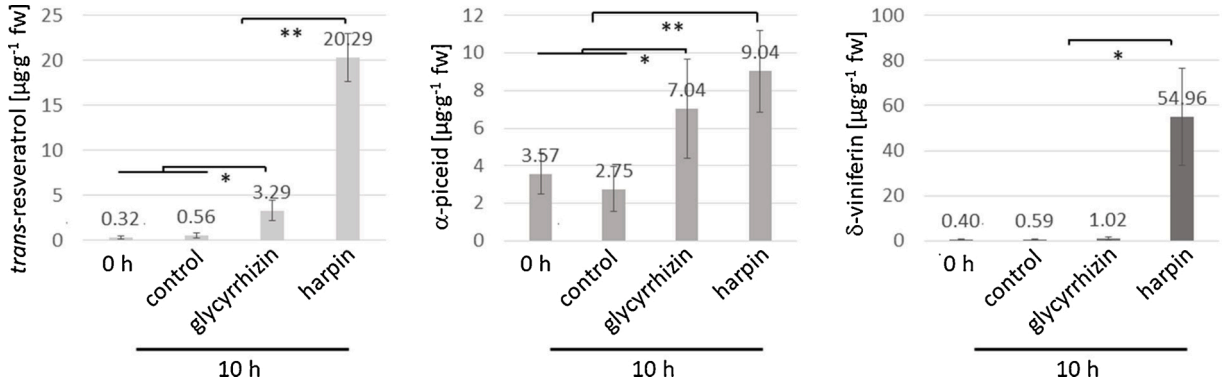

Fig. 6. Glycyrrhizin can induce the accumulation of glycosylated stilbenes in suspension cells of *Vitis rupestris*. Accumulation of the aglycon trans-resveratrol (left), the glycosylated stilbene *trans*-piceid (center), and the oxidised dimer δ-viniferin (right) in µg per g fresh weight prior to (0 h) and 10 h after addition of either 100 µM glycyrrhizin or 9 $\mu g \cdot ml^{-1}$ of the bacterial elicitor harpin (as positive control). Data represent mean values and standard errors from at least three independent biological replicates. Statistical significance was assessed using a student *t*-test with defining *as $P \leq 0.05$, and as **$P \leq 0.01$.

the microscope stage, were maintaining their overall configuration (Fig. 7A). In contrast, treatment with 20 µM glycyrrhizin elicited a massive change of actin structure that was already significant at the first possible time point of observation (5 min after adding the compound, mounting the specimen, and adjusting the spinning-disc microscope). Here, bright fluorescent actin speckles were seen in the cell centre around the nucleus in addition to the usual filaments in the cortex (Fig. 7B). In the subsequent time points, these speckles increased in brightness, while the peripheral actin filaments became depleted. Compared to the situation in tobacco BY-2 cells (Fig. 1), the actin cytoskeleton of the grapevine cells appeared to be more sensitive to modulation. Since already the mere observation on a slide under the microscope was able to induce actin bundling (similar to the situation in tobacco cells after treatment with glycyrrhizin, compare Fig. 1B with Fig. 7A), while in grapevine cells glycyrrhizin induced a much stronger actin contraction towards the nucleus culminating in perinuclear speckles.

To test, whether this actin contraction response to glycyrrhizin can be observed in real plant tissue, we used leaf discs excised from leaves of the *V. vinifera* cv. Chardonnay plant expressing the fluorescent actin marker *GFP-AtFABD2*, and followed the actin responses in epidermal cells at the adaxial (upper) and abaxial (lower) side of the disc by confocal spinning disc microscopy. Due to the presence of impermeable cuticles, we had to increase the concentration of glycyrrhizin considerably. In the abaxial side, where the stomata are located, we were able to trigger a massive contraction of actin, which was much more pronounced as compared to the suspension cells (Fig. 8A). In the guard cells, several agglomerations of actin around the chloroplasts were seen, while in the neighbouring epidermal pavement cells became more or less eliminated. To investigate this response in a quantitative manner, we used the skewness of the intensity histogram as readout, since redistribution of a signal from a homogenous to a condensed distribution will result in overrepresentation of low-intensity pixels, while pixels of high intensity will not increase to the same extent due to signal saturation. This optical phenomenon, which also is known as sieve effect, will, therefore, produce an asymmetry of the histogram to the left side, which can be used to measure actin condensation [45]. Since the actin response in the abaxial side was especially strong in guard cells, we conducted the quantification separately for pavement cells and guard cells (Fig. 8B). While a lower concentration of glycyrrhizin (2 mM) or treatment with water as solvent control increased the skew only insignifantly for pavement cells, 4 mM caused a significant increase. For guard cells, the response to glycyrrhizin was more sensitive – here, already for 2 mM of glycyrrhizin, the skew increased significantly, and for 4 mM, the effect was increased further.

In contrast, in the adaxial side, while seeing a certain actin response as well, mirrored by a progressive increase of the skew, we could only detect an apparent difference between 4 mM glycyrrhizin treatment and solvent control (15 min), and the response was less pronounced as compared to the abaxial side. We have to mention that the observation of the adaxial side required that the abaxial side with the stomata was facing the slide and therefore was imbibed with water (needed to avoid drying of the sample), such that air exchange through the stomata was impaired. In contrast, for observation of the abaxial side, the stomata

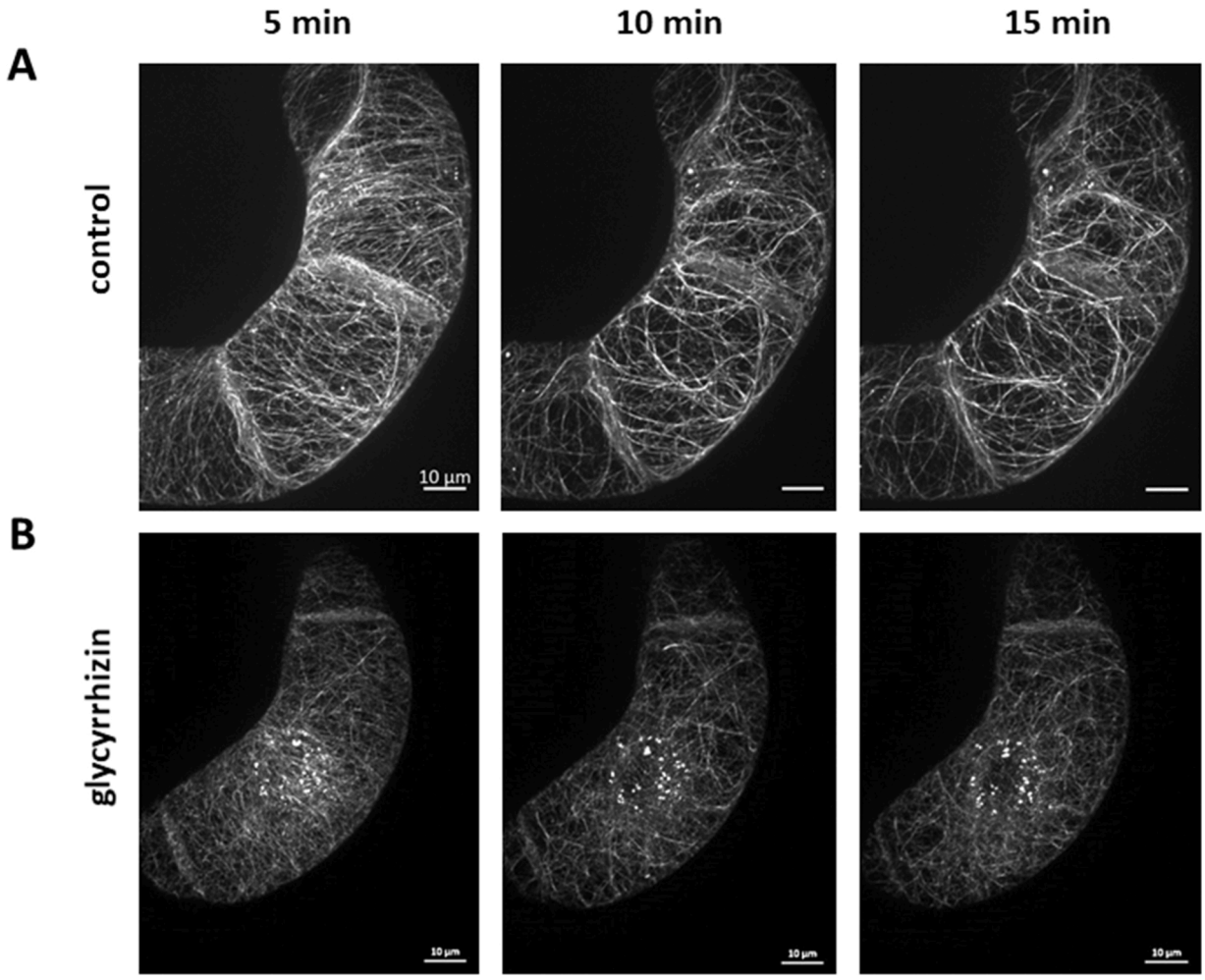

Fig. 7. Response of actin filaments to glycyrrhizin in non-cycling cells from *V. vinifera* cv. Chardonnay expressing the actin marker fimbrin actin-binding domain 2 in fusion with GFP. **A** control cells treated with water, **B** cells treated with 20 µM of glycyrrhizin. Geometric projections of confocal z-stacks are shown. Size bar corresponds to 10 µm.

were facing upwards and therefore were not imbibed. This experimental limitation (which could not be avoided) should be kept in mind because it bears upon the interpretation (given below in the discussion), why we did not observe any significant actin response in the adaxial side, while actin was responding during the observation of the abaxial side.

4. Discussion

Traditional approaches to controlling pathogens in grapevines have several limitations and problems. Therefore, new approaches are required. The current study was intended as contribution to explore the potential of defence priming as an alternative method. As previous studies had shown that glycyrrhizin could induce actin reorganisation through ROS in animal cells and even in Oomycete zoospores, the relationship between ROS and actin seems to be evolutionarily conserved in eukaryotic cells. Since this ROS-actin circuit seems to act as a system to detect perturbations of membrane integrity, and, thus, might be used as a trigger of plant defence [24,27]. Thus, we predict that in plant cells, glycyrrhizin can also induce defence responses. In the current study, we tested several implications of this hypothesis, such as actin remodelling, its dependence on the activity of the NADPH oxidase RboH and auxin, the activation of phytoalexin synthesis genes, the accumulation of stilbene phytoalexins, as well as induction of cell death by glycyrrhizin, making use of transgenic grapevine cells and plants expressing a fluorescent actin marker. We will now briefly address methodological aspects of analysing actin remodelling in cells and leaves, then discuss potential mechanisms for the modulation of actin remodelling by glycyrrhizin, continue with the downstream events including activation of phytoalexin synthesis genes, and potential posttranslational regulation of stilbene accumulation, and then develop a working model, from which we derive implications for future research.

4.1. How to quantify actin reorganisation

To quantify actin reorganisation is a difficult task, due to the high complexity of actin arrays that differ in several aspects, such as bundling, orientation, waviness, and dynamicity (see [24], for discussion of this parameter). Several methods to quantify this complexity have been proposed [46,52], however, none of these methods can be generalised, due to the impressive diversity of actin arrays in different cell types, and in response to different signals. Therefore, each strategy has to be tailored to the respective system. The defence response of actin in suspension cells consists of three concomitant events – cortical filaments are depleted, while perinuclear filaments are bundled, and, third, actin filaments contract to the nucleus. To quantify the bundling is possible by measuring profiles of intensity along a probing line and calculating from those changes in actin thickness. However, in the case of glycyrrhizin, these differences are relatively small, and their quantification turns out to be quite cumbersome. Also the second defence-related phenomenon, depletion of actin filaments from the cell

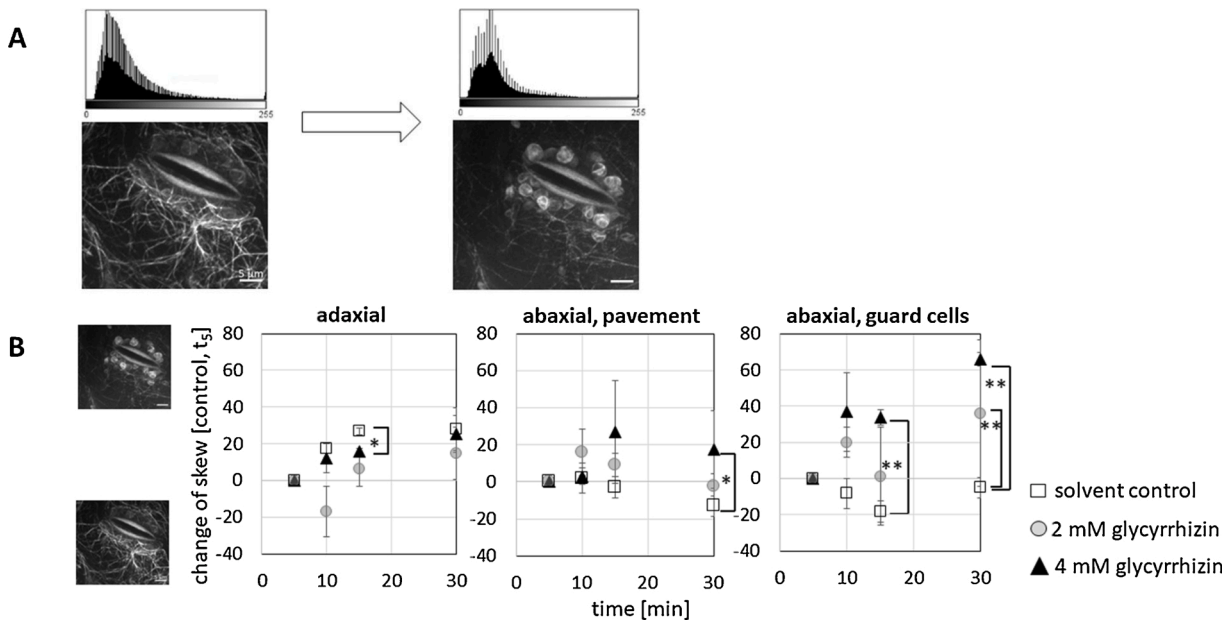

Fig. 8. Response of actin filaments to glycyrrhizin in leaf discs from *V. vinifera* cv. Chardonnay expressing the actin marker fimbrin actin-binding domain 2 in fusion with GFP. **A** representative example of nuclear actin contraction in abaxial cells leading to a shift in the intensity histogram that can be quantified by a change of the skew. Size bar corresponds to 5 µm. **B** change of skew on the adaxial (left-hand graph) and abaxial (central and right-hand graphs) face of leaf discs either treated with water as solvent control (open squares), with 2 mM glycyrrhizin (grey circles) or with 4 mM glycyrrhizin (black triangles). For the abaxial side, change of skew was determined separately for pavement cells (central graph) and guard cells (right-hand graph). Data represent mean values and standard errors from at least three independent biological replicates. Statistical significance was assessed using a student *t*-test with defining *as $P \leq 0.05$, and as **$P \leq 0.01$.

cortex, while yielding significant differences, turned out to be time-consuming as well. It turned out that the third aspect, the contraction of actin on the nucleus, was much easier to be scored (Fig. 2). During a preparatory study, we have compared the results obtained from scoring cortical depletion and from central contraction with the same set of cells and obtained similar results (Suppl. Fig. S2). However, the approach to score central contraction required only 25 % of the time and also turned out to be more robust against fluctuations between individual cells. Therefore, the method of quantifying the central contraction of actin was later employed to conduct this study.

Also in leaf discs of grapevine expressing the actin marker *AtFABD2*, actin contracts around the nucleus in response to pathogens or in response to activation of defence by elicitors. In principle, one might therefore quantify this in each individual cell in the same way as discussed above. However, this turned out to be very cumbersome and time-consuming, because the cells are smaller, cell borders were more difficult to delineate, the cells were of different types (guard cells and pavement cells),and cells of different orientation are intertwined. We, therefore, relied upon a strategy introduced by Higaki, Kutsuna, Sano and Hasezawa [46], measuring changes in skew of the intensity histogram as readout. While in the original protocol, the skew was used to estimate actin bundling, it should be said explicitly that bundling is not the only actin response that would bear on the skew, since any change of actin distribution, where diffuse signals are contracted, would cause a shift of the skew. So, we used this strategy to infer the degree the condensation of actin upon the nucleus. While the skew turned out to reflect the visual impression of actin remodelling, in our hands, this approach suffered from considerable noise, when snapshots from different leaf regions are compared. However, it worked reliably, when a given region of interest was followed over time, because the influences of static structures, such as cell walls, on the skew remain constant and will not bear on the differential of the skew. Summarising, to our experience, quantifications of actin have to be adjusted to the respective system, and have to be calibrated by using time series of the same region of interest. It is also not making any sense to compare absolute numbers obtained from different cell types or tissues, one can only rely on relative changes to compare different conditions or treatments of the same cell type or tissue.

4.2. *Glycyrrhizin might trigger an evolutionary ancient sensor for membrane integrity*

Rapid reorganisation of the actin cytoskeleton at the infection site has been observed as early plant response to fungal or oomycete pathogens [53–56]. The function of this response has been suggested to relate to vesicle transport towards the penetration site, critical for the formation of cell wall appositions and the accumulation of antimicrobial compounds [57]. This actin function is basically of structural nature.

There is, however, accumulating evidence that cortical actin filaments are not only acting as structural “skeleton”, but convey sensory functions. Such sensory functions of actin are well described in animal cells, for instance for mechanosensing during migration of mammalian cells (reviewed in [58,59]). In plants, as well, many external signals are perceived and transduced from the cell wall to the cytoskeleton (reviewed in [60]). In particular, a membrane-associated subpopulation of actin takes part in the regulation of membrane dynamics [61], and sustains membrane integrity during volume regulation [62]. Perturbations of membrane integrity are followed by rapid detachment of cortical actin and formation of actin cables [27], depending on leakage of apoplastic reactive oxygen species generated by the plasma-membrane located NADPH oxidase Respiratory burst oxidase Homologue [24].

The working hypothesis that glycyrrhizin triggers this membrane integrity sensor can explain several findings of the current study: 1. Actin remodelling in response to glycyrrhizin can be suppressed by diphenylene iodonium, a specific inhibitor of Respiratory burst oxidase Homologue (Fig. 2B), consistent to results obtained with other membrane disrupters, such as the bacterial elicitor harpin [27], or the cell-penetrating peptide BP100 [24]. 2. Mortality induced by glycyrrhizin can be mitigated by indole-acetic acid (Fig. 3), a transportable auxin that can suppress actin remodelling in response to perturbed membrane integrity [24,27]. 3. The sensitivity of cell cycling and

induction of cell death is significantly reduced in cells, where actin dynamics are reduced by overexpression of the fimbrin actin-binding domain (Fig. 3).

This actin-ROS based membrane integrity sensor seems to be evolutionarily ancient, because some of its characteristic features and players have also been described for animal cells: For instance, upon induction of cell migration and phagocytosis (both responses are relevant for their immunity) three cytosolic subunits of the plasma-membrane located NADPH oxidase complex, p40-phox, p47-phox, and p67-phox, bind to actin filaments [63]. This process involves other actin-binding proteins (such as cofilin and coronin), demonstrating a strong link between innate immunity, ROS production/signalling and the actin cytoskeleton. There is also evidence that glycyrrhizin targets this functional circuit in animal cells as well. For example, glycyrrhetinic acid, an aglycone of glycyrrhizin, induced disruption of F-actin in mouse tumour cells [64]. On the other hand, ammonium glycyrrhizinate, an ammonium salt of glycyrrhizin, was shown to block potently H_2O_2-induced actin disruption in gastric epithelial cells [65]. Into the same direction points the observation that glycyrrhizin can mitigate inflammations by suppressive oxidative burst [39]. Also in zoospores of the Oomycete *Plasmopara viticola*, glycyrrhizin induced cell burst depending on actin and the plasma membrane located NADPH oxidase [31]. Thus, the link between actin and ROS generated by plasma-membrane located NADPHS oxidases seems to be evolutionarily ancient. Our data are consistent with the assumption that this functional circuit, which is probably linked with sensing of membrane integrity, is also preserved in cells of higher plants.

4.3. The actin-ROS membrane integrity sensor can trigger defence

We pursue the hypothesis that glycyrrhizin can trigger the actin-ROS sensor for membrane integrity. This hypothesis leads to the implication that specific glycyrrhizin-induced defence responses must exist. In fact, we could show in this study that glycyrrhizin stimulated apoplastic alkalinisation, expression of phytoalexin genes, and the accumulation of glycosylated stilbenes. These results support the idea that actin bundling is a shift signal from growth to defence.

There are specific differences, though: While transcripts of *PAL* and *RS* (Fig. 5) were induced strongly, the response of *StSy* was much slower and weaker although the encoded gene product is expected to catalyse the same reaction as RS, namely, synthesis of the stilbene aglycone resveratrol. However, the stilbene synthases are organised in a large gene family, with different clades that differ in their regulation pattern and might be under control of different transcription factors [66]. The induction of resveratrol-synthase transcripts was followed by a mild accumulation of *trans*-resveratrol, and a more substantial accumulation of its glycosylated derivative α-piceid (Fig. 6), indicative of a scenario, where the newly formed stilbene aglycone is rapidly linked with a glucose moiety. In contrast, δ-viniferine, one of the oxidised resveratrol oligomers, did not accumulate. The glycosylated α-piceid shows only weak antifungal activity and might represent a storage pool, while the aglycone *trans*-resveratrol and, to a higher extent, the viniferins, are potent antimicrobial compounds [67,68]. In a comparative study in of defence responses triggered in grapevine cells by the PAMP flg22 and the cell-death inducing elicitor harpin, the accumulation of *trans*--resveratrol and δ-viniferine was found to be a hallmark for cell-death related defence, while accumulation of α-piceid marked basal immunity [13]. Also in our work, glycyrrhizin (in contrast to harpin) failed to induce any δ-viniferine, which would support a scenario that the type of defence induced by glycyrrhizin classifies as basal immunity. However, on the other hand, we observed that a significant fraction of the cells had undergone cell death, when scored 48 h after addition of glycyrrhizin (Suppl. Fig. S3). The mortality is comparable to that seen for treatment with harpin [27], and also to that found in tobacco BY-2 cells (Fig. 3C), supporting a scenario, where the defence response evoked by glycyrrhizin is of the cell-death related type. Even though the glucoside α-piceid is not directly toxic for fungal pathogens, it may be related to plant defence priming responses: Storage of glycosylated metabolites in the vacuole could be seen as anticipative strategy, which under pathogen attack would allow for rapid release of bioactive phytoalexins following cleavage of the sugar moiety [23].

4.4. Actin as a switch for cell-death related immunity?

In order to cope with unfavourable conditions, plants have to repartition their resources between defence and growth in a balanced and regulated manner [69]. We pursue the working hypothesis that this balance is regulated by the cortical actin cytoskeleton. This hypothesis implies that addition of auxin should reduce defence-related remodelling of actin as well as defence responses. This had been demonstrated in previous work for tobacco BY-2 cells [24], but also for grapevine cells [27]. Also in the current study, auxin can mitigate the induction of mortality by glycyrrhizin (Fig. 3C). Interestingly, the delay of cell cycling, the same holds true for the mortality response, is much weaker in GF11 cells as compared to non-transformed BY-2 cells (Fig. 3). This may due to a mild reduction of actin dynamics caused by the overexpression of the *AtFABD2* marker [42], and provides evidence for a causative role of actin remodelling for the cellular responses to glycyrrhizin.

Thus, the phenomenon is related to the balance between auxin and glycyrrhizin. Since glycyrrhizin-induced actin remodelling can be suppressed by diphenylene iodonium (Fig. 2), a specific inhibitor of the NADPH oxidase Respiratory burst oxidase Homologue (RboH), the balance between auxin and glycyrrhizin might be established by their competition for the common signalling molecule superoxide, which can regulate actin organisation by a mechanism involving phospholipase D, and phosphatidyl inositol-4,5-bisphosphate (PIP2) that modulate actin remodelling by sequestering actin modifiers, such as actin-depolymerisation factors and capping proteins [24].

The activation of RboH-dependent actin remodelling produces two cellular readouts: activation of phytoalexin genes, and cell death. These cellular responses can be mitigated by auxin and diphenylene iodonium (Figs. 2 and 3; [24,27]), concomitant with respective effects on actin remodelling. The accumulation of ROS in response to glycyrrhizin and the inhibition of this accumulation by diphenylene iodonium was not experimentally addressed in the current study. However, previous studies for grapevine cells have shown (i) that activation of defence genes by the bacterial elicitor harpin is preceded by the accumulation of cytoplasmic ROS [13]; (ii) that RboH activity is necessary for harpin-triggered gene activation [28]; and (iii) that actin bundling in response to harpin requires RboH activity [27]. The most straightforward way is a working model (Fig. 9) where actin remodelling (triggered by RboH-dependent ROS) is upstream of defence signalling. In addition to RboH-dependent actin remodelling, glycyrrhizin also activates a calcium influx (Fig. 4), a hallmark of MAMP-triggered basal immunity (reviewed in [70]). The almost instantaneous activation of alkalinisation by high concentrations of glycyrrhizin (Fig. 4A) points to a direct activation (rather than indirectly through activation of calcium channels by apoplastic ROS, [71]). In the same cellular model, the phytoalexin genes are induced in a similar manner for both MAMP-triggered immunity (experimentally triggered by flg22) that is not accompanied by cell death, and for harpin-triggered immunity that is linked with cell death [13]. Thus, these two cellular responses (activation of phytoalexins synthesis genes and cell death) can be uncoupled and, therefore, must be mediated by different pathways (Fig. 9, ⑤). In grapevine, the activation of defence-related cell death is linked with the activation of metacaspase 2 and 5 [72]. It remains to be elucidated, whether both inputs (calcium influx, actin remodelling) are needed for this cellular response. It is also interesting that glycyrrhizin seems to activate specifically the stilbene synthases addressed by the RS primer, while other members of this gene family [66] that are addressed by the StSy primer, are less responsive.

The role of actin remodelling as signalling event that can steer

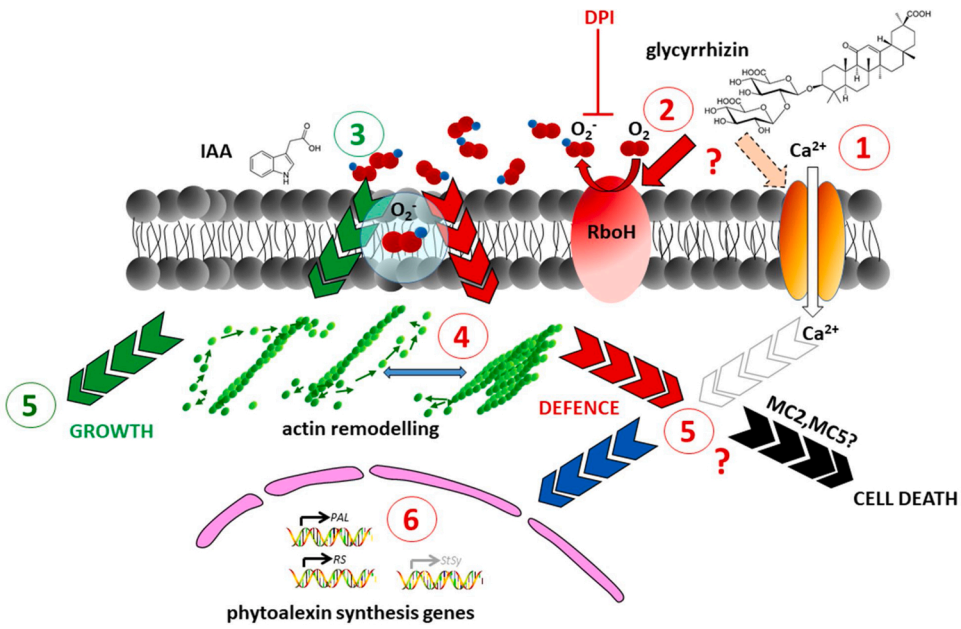

Fig. 9. Working model for the effect of glycyrrhizin on plant defence. Interaction of glycyrrhizin with the membrane (through a specific binding site?) will activate calcium influx ( ), as well as the NADPH oxidase Respiratory burst oxidase Homologue (RboH, ②), a process that can be inhibited by diphenylene iodonium (DPI). The resulting apoplastic superoxide ions (③) convey a signal through the membrane that controls the organisation of cortical actin filaments (④). Superoxide ions are also used to mediate the effect of auxin on a dynamic actin configuration that supports growth (⑤). Since the abundance of superoxide is limited, defence- and growth-related signalling compete. The defence signal deployed by the RboH-generated apoplastic oxidative burst is merging downstream of actin (⑤) with the calcium-dependent signal that activates phytoalexins genes (⑥). This merge activates a machinery, possibly involving metacaspases 2 and 5, that culminates in programmed cell death. Question marks indicate future research topics.

different readouts of plant defence would lead to the implication that this remodelling should be specifically pronounced in cells, where pathogen entry is to be expected. Many pathogens, for instance the oomycete *Plasmopara viticola* (the causative agent of Downy Mildew of Grapevine) specifically target to the stomata for host colonisation [73]. Guard cell actin responds to this pathogen with a strong condensation upon the nucleus, and this accompanied by a similar response to the pavement cells, although the pathogen has not attached to those cells directly [44]. This has led to the concept of a gatekeeper function of guard cell actin. Glycyrrhizin seems to be able to mimick the actin response to *P. viticola* with respect to guard cells (Fig. 8B). Since glycyrrhizin does not cause a similar actin response in the pavement cells, the systemic "gatekeeper signal" seems to require additional factors deriving from the pathogen (possibly surface structures that can act as elicitors).

4.5. Outlook

The current work demonstrates that glycyrrhizin could induce defence responses in grapevine cells by causing actin remodelling. Whether these glycyrrhizin-induced responses will culminate in a priming memory has not been addressed here, because it would require a different experimental design, where the cells or leaves are challenged by pathogens following a pretreatment with glycyrrhizin. This remains to be addressed in future works. From the model (Fig. 9), two additional questions emerge: (1) Is glycyrrhizin binding to a receptor, and if so, is the receptor triggering oxidative burst and actin remodelling identical to that, which is responsible for calcium influx? (2) At what stage of defence signalling does the pathway leading to cell death diverge from basal immunity? How does this bifurcation depend on actin remodelling? One way to approach these questions is to search for other triggers that possibly allow to uncouple actin remodelling from cell death.

Declaration of Competing Interest

The authors report no declarations of interest.

Acknowledgements

This work was supported by a fellowship from the Chinese Scholarship Council to Hao Wang, and funds from the Interreg Upper Rhine project Vitifutur.

This publication uses data collected within the framework of the PhD thesis 'The TCM drug Gan Cao stimulates defence in grapevine' of Hao Wang published in 2019 at the faculty of Chemistry and Biosciences, Karlsruhe Institute of Technology. dio: 10.5445/IR/1000095236.

Appendix A. Supplementary data

Supplementary material related to this article can be found, in the online version, at doi:https://doi.org/10.1016/j.plantsci.2020.110712.

References

[1] S. Myles, A.R. Boyko, C.L. Owens, P.J. Brown, F. Grassi, M.K. Aradhya, B. Prins, A. Reynolds, J.M. Chia, D. Ware, C.D. Bustamante, E.S. Buckler, Genetic structure and domestication history of the grape, Proc. Natl. Acad. Sci. U. S. A. 108 (2011) 3530–3535.
[2] Eurostat, 2000 available under, ec.europa.eu/eurostat/documents/3217494.
[3] F. Giraud, D. Molitor, M. Bleunven, D. Evers, Fungicide sensitivity profiles of the *Plasmopara viticola* populations in the Luxembourgian grape-growing region, J. Plant Pathol. S1 (2013) 55–62.
[4] G. Bleyer, H. Kassemeyer, M. Breuer, R. Krause, O. Viret, P. Dubuis, A. Fabre, B. Bloesch, W. Siegfried, A. Naef, "VitiMeteo" - a future-oriented forecasting system for viticulture, IOBC/WPRS Bull. 67 (2011) 69–77.
[5] R. Eibach, E. Zyprian, L. Welter, R. Toepfer, The use of molecular markers for pyramiding resistance genes in grapevine breeding, Vitis 46 (2007) 120–124.
[6] J.D.G. Jones, J.L. Dangl, The plant immune system, Nature 444 (2006) 323–329.
[7] E.M. Reimer-Michalski, U. Conrath, Innate immune memory in plants, Semin. Immunol. 28 (2016) 319–327.
[8] C. Zipfel, G. Kunze, D. Chinchilla, A. Caniard, J.D.G. Jones, T. Boller, G. Felix, Perception of the bacterial PAMP EF-Tu by the receptor EFR restricts Agrobacterium-mediated transformation, Cell 125 (2006) 749–760.
[9] Y. Tao, Z.Y. Xie, W.Q. Chen, J. Glazebrook, H.S. Chang, B. Han, T. Zhu, G.Z. Zou, F. Katagiri, Quantitative nature of Arabidopsis responses during compatible and incompatible interactions with the bacterial pathogen Pseudomonas syringae, Plant Cell 15 (2003) 317–330.
[10] L. Navarro, C. Zipfel, O. Rowland, I. Keller, S. Robatzek, T. Boller, J.D.G. Jones, The transcriptional innate immune response to flg22. interplay and overlap with*Avr* gene-dependent defense responses and bacterial pathogenesis, Plant Physiol. 135 (2004) 1113–1128.
[11] K. Tsuda, F. Katagiri, Comparing signaling mechanisms engaged in pattern-triggered and effector-triggered immunity, Curr. Opin. Plant Biol. 13 (2010) 459–465.
[12] R.A. Caldo, D. Nettleton, R.P. Wise, Interaction-dependent gene expression in Mla-specified response to barley powdery mildew, Plant Cell 16 (2004) 2514–2528.
[13] X.L. Chang, P. Nick, Defence signalling triggered by Flg22 and harpin is integrated into a different stilbene output in *Vitis* cells, PLoS One 7 (2012), e40446.
[14] L.M. Dai, D. Wang, X.Q. Xie, C.H. Zhang, X.P. Wang, Y. Xu, Y.J. Wang, J.X. Zhang, The novel gene *VpPR4-1* from *Vitis pseudoreticulata* increases powdery mildew resistance in transgenic *Vitis vinifera* l, Front. Plant Sci. 7 (2016) 12.

[15] Y.T. Jiao, W.R. Xu, D. Duan, Y.J. Wang, P. Nick, A stilbene synthase allele from a Chinese wild grapevine confers resistance to powdery mildew by recruiting salicylic acid signalling for efficient defence, J. Exp. Bot. 67 (2016) 5841–5856.
[16] S. Schröder, A. Kortekamp, E. Heene, J. Daumann, I. Valea, P. Nick, Crop wild relatives as genetic resources–the case of the European wild grape, Can. J. Plant Sci. 95 (2015) 905–912.
[17] D. Duan, D. Halter, R. Baltenweck, C. Tisch, V. Troster, A. Kortekamp, P. Hugueney, P. Nick, Genetic diversity of stilbene metabolism in *Vitis sylvestris*, J. Exp. Bot. 66 (2015) 3243–3257.
[18] D. Duan, S. Fischer, P. Merz, J. Bogs, M. Riemann, P. Nick, An ancestral allele of grapevine transcription factor MYB14 promotes plant defence, J. Exp. Bot. 67 (2016) 1795–1804.
[19] S. Fröbel, J. Dudenhöffer, R. Töpfer, E. Zyprian, Transcriptome analysis of early downy mildew (*Plasmopara viticola*) defense in grapevines carrying the Asian resistance locus *Rpv10*, Euphytica 215 (2019) 28.
[20] U. Conrath, G.J.M. Beckers, V. Flors, P. Garcia-Agustin, G. Jakab, F. Mauch, M. A. Newman, C.M.J. Pieterse, B. Poinssot, M.J. Pozo, A. Pugin, U. Schaffrath, J. Ton, D. Wendehenne, L. Zimmerli, B. Mauch-Mani, A.P.G. Prime, Priming: Getting ready for battle, Mol. Plant-Microbe Interact. 19 (2006) 1062–1071.
[21] S. Ahmad, R. Gordon-Weeks, J. Pickett, J. Ton, Natural variation in priming of basal resistance: from evolutionary origin to agricultural exploitation, Mol. Plant Pathol. 11 (2010) 817–827.
[22] U. Conrath, Molecular aspects of defence priming, Trends Plant Sci. 16 (2011) 524–531.
[23] V. Pastor, E. Luna, B. Mauch-Mani, J. Ton, V. Flors, Primed plants do not forget, Environ. Exp. Bot. 94 (2013) 46–56.
[24] K. Eggenberger, P. Sanyal, S. Hundt, P. Wadhwani, A.S. Ulrich, P. Nick, Challenge integrity: the cell-penetrating peptide BP100 interferes with the auxin-actin oscillator, Plant Cell Physiol. 58 (2017) 71–85.
[25] F. Qiao, X.L. Chang, P. Nick, The cytoskeleton enhances gene expression in the response to the Harpin elicitor in grapevine, J. Exp. Bot. 61 (2010) 4021–4031.
[26] X. Guan, G. Buchholz, P. Nick, The cytoskeleton is disrupted by the bacterial effector HrpZ, but not by the bacterial PAMP flg22, in tobacco BY-2 cells, J. Exp. Bot. 64 (2013) 1805–1816.
[27] X. Chang, M. Riemann, Q. Liu, P. Nick, Actin as deathly switch? How auxin can suppress cell-death related defence, PLoS One 10 (2015), e0125498.
[28] X. Chang, E. Heene, F. Qiao, P. Nick, The phytoalexin resveratrol regulates the initiation of hypersensitive cell death in *Vitis* cell, PLoS One 6 (2011), e26405.
[29] M. Koivusalo, A. Kapus, S. Grinstein, Sensors, Transducers, and Effectors That Regulate Cell Size and Shape, J. Biol. Chem. 284 (2009) 6595–6599.
[30] P. Hohenberger, C. Eing, R. Straessner, S. Durst, W. Frey, P. Nick, Plant actin controls membrane permeability, Biochim. Biophys. Acta-Biomembr. 1808 (2011) 2304–2312.
[31] V. Tröster, T. Setzer, T. Hirth, A. Pecina, A. Kortekamp, P. Nick, Probing the contractile vacuole as Achilles' heel of the biotrophic grapevine pathogen *Plasmopara viticola*, Protoplasma 254 (2017) 1887–1901.
[32] M.J. Deeks, J.R. Calcutt, E.K.S. Ingle, T.J. Hawkins, S. Chapman, A.C. Richardson, D.A. Mentlak, M.R. Dixon, F. Cartwright, A.P. Smertenko, K. Oparka, P.J. Hussey, A superfamily of actin-binding proteins at the actin-membrane nexus of higher plants, Curr. Biol. 22 (2012) 1595–1600.
[33] J.L. Henty-Ridilla, M. Shimono, J.J. Li, J.H. Chang, B. Day, C.J. Staiger, The plant actin cytoskeleton responds to signals from microbe-associated molecular patterns, PLoS Pathog. 9 (2013) 13.
[34] J.L. Henty-Ridilla, J.J. Li, B. Day, C.J. Staiger, ACTIN DEPOLYMERIZING FACTOR4 regulates actin dynamics during innate immune signaling in *Arabidopsis*, Plant Cell 26 (2014) 340–352.
[35] V.E. Franklin-Tong, C.W. Gourlay, A role for actin in regulating apoptosis/programmed cell death: evidence spanning yeast, plants and animals, Biochem. J. 413 (2008) 389–404.
[36] S.G. Liu, D.Z. Zhu, G.H. Chen, X.Q. Gao, X.S. Zhang, Disrupted actin dynamics trigger an increment in the reactive oxygen species levels in the Arabidopsis root under salt stress, Plant Cell Rep. 31 (2012) 1219–1226.
[37] J.J. Li, L.Y. Cao, C.J. Staiger, Capping protein modulates actin remodeling in response to reactive oxygen species during plant innate immunity, Plant Physiol. 173 (2017) 1125–1136.
[38] F. Waller, Phytotherapie der traditionellen chinesischen Medizin, Zeitschrift für Phytotherapie 19 (1998) 77–91.
[39] M.N. Asl, H. Hosseinzadeh, Review of pharmacological effects of Glycyrrhiza sp and its bioactive compounds, Phytother. Res. 22 (2008) 709–724.
[40] T. Nagata, Y. Nemoto, S. Hasezawa, Tobacco BY-2 cell line as the "HeLa" cell in the cell biology of higher plants, Int. Rev. Cytol. 132 (1992) 1–30.
[41] T. Sano, T. Higaki, Y. Oda, T. Hayashi, S. Hasezawa, Appearance of actin microfilament 'twin peaks' in mitosis and their function in cell plate formation, as visualized in tobacco BY-2 cells expressing GFP-fimbrin, Plant J. 44 (2005) 595–605.
[42] X. Huang, J. Maisch, P. Nick, Sensory role of actin in auxin-dependent responses of tobacco BY-2, J. Plant Physiol. 218 (2017) 6–15.
[43] T. Seibicke, Untersuchungen zur induzierten Resistenz an *Vitis spec*, University of Freiburg, 2002.
[44] X. Guan, G. Buchholz, P. Nick, Actin marker lines in grapevine reveal a gatekeeper function of guard cells, J. Plant Physiol. 171 (2014) 1164–1173.
[45] T. Higaki, N. Kutsuna, T. Sano, N. Kondo, S. Hasezawa, Quantification and cluster analysis of actin cytoskeletal structures in plant cells: role of actin bundling in stomatal movement during diurnal cycles in Arabidopsis guard cells, Plant J. 61 (2010) 156–165.
[46] T. Higaki, N. Kutsuna, T. Sano, S. Hasezawa, Quantitative analysis of changes in actin microfilament contribution to cell plate development in plant cytokinesis, BMC Plant Biol. 8 (2008) 15.
[47] D. Gaff, O. Okong'O-Ogola, The use of non-permeating pigments for testing the survival of cells, J. Exp. Bot. 22 (1971) 756–758.
[48] G. Felix, M. Regenass, T. Boller, Specific perception of subnanomolar concentrations of chitin fragments by tomato cells: induction of extracellular alkalinization, changes in protein phosphorylation, and establishment of a refractory state, Plant J. 4 (1993) 307–316.
[49] K.E. Reid, N. Olsson, J. Schlosser, F. Peng, S.T. Lund, An optimized grapevine RNA isolation procedure and statistical determination of reference genes for real-time RT-PCR during berry development, BMC Plant Biol. 6 (2006) 27.
[50] K.J. Livak, T.D. Schmittgen, Analysis of relative gene expression data using real-time quantitative PCR and the 2(T)(-Delta Delta C) method, Methods 25 (2001) 402–408.
[51] J. Maisch, P. Nick, Actin is involved in auxin-dependent patterning, Plant Physiol. 143 (2007) 1695–1704.
[52] A.P. Smertenko, M.J. Deeks, P.J. Hussey, Strategies of actin reorganisation in plant cells, J. Cell. Sci. 123 (2010) 3019–3029.
[53] B. Day, J.L. Henty, K.J. Porter, C.J. Staiger, The pathogen-actin connection: a platform for defense signaling in plants, Annu. Rev. Phytopathol. 49 (2011) 483–506.
[54] K.S. Opalski, H. Schultheiss, K.H. Kogel, R. Huckelhoven, The receptor-like MLO protein and the RAC/ROP family G-protein RACB modulate actin reorganization in barley attacked by the biotrophic powdery mildew fungus *Blumeria graminis f.sP hordei*, Plant J. 41 (2005) 291–303.
[55] I. Kobayashi, Y. Kobayashi, A.R. Hardham, Dynamic reorganization of microtubules and microfilaments in flax cells during the resistance response to flax rust infection, Planta 195 (1994) 237–247.
[56] D. Takemoto, D.A. Jones, A.R. Hardham, Re-organization of the cytoskeleton and endoplasmic reticulum in the Arabidopsis pen1-1 mutant inoculated with the non-adapted powdery mildew pathogen, *Blumeria graminis f. sp hordei*, Mol. Plant Pathol. 7 (2006) 553–563.
[57] A.R. Hardham, D.A. Jones, D. Takemoto, Cytoskeleton and cell wall function in penetration resistance, Curr. Opin. Plant Biol. 10 (2007) 342–348.
[58] P.A. Janmey, D.A. Weitz, Dealing with mechanics: mechanisms of force transduction in cells, Trends Biochem. Sci. 29 (2004) 364–370.
[59] A.W. Orr, B.P. Helmke, B.R. Blackman, M.A. Schwartz, Mechanisms of mechanotransduction, Dev. Cell 10 (2006) 11–20.
[60] C. Thomas, Bundling actin filaments from membranes: some novel players, Front. Plant Sci. 3 (2012) 14.
[61] M.J. Deeks, M. Fendrych, A. Smertenko, K.S. Bell, K. Oparka, F. Cvrckova, V. Zarsky, P.J. Hussey, The plant formin AtFH4 interacts with both actin and microtubules, and contains a newly identified microtubule-binding domain, J. Cell. Sci. 123 (2010) 1209–1215.
[62] Q. Liu, F. Qiao, A. Ismail, X.L. Chang, P. Nick, The plant cytoskeleton controls regulatory volume increase, Biochim. Biophys. Acta-Biomembr. 1828 (2013) 2111–2120.
[63] T. Kobayashi, S. Tsunawaki, H. Seguchi, Evaluation of the process for superoxide production by NADPH oxidase in human neutrophils: evidence for cytoplasmic origin of superoxide, Redox Rep. 6 (2001) 27–36.
[64] H. Yamaguchi, T. Noshita, T. Yu, Y. Kidachi, K. Kamiie, H. Umetsu, K. Ryoyama, Novel effects of glycyrrhetinic acid on the central nervous system tumorigenic progenitor cells: induction of actin disruption and tumor cell-selective toxicity, Eur. J. Med. Chem. 45 (2010) 2943–2948.
[65] H.M. Oh, S. Lee, Y.N. Park, E.J. Choi, J.Y. Choi, J.A. Kim, J.H. Kweon, W.C. Han, S. C. Choi, J.K. Han, J.K. Son, S.H. Lee, C.D. Jun, Ammonium glycyrrhizinate protects gastric epithelial cells from hydrogen peroxide-induced cell death, Exp. Biol. Med. 234 (2009) 263–277.
[66] A. Vannozzi, I.B. Dry, M. Fasoli, S. Zenoni, M. Lucchin, Genome-wide analysis of the grapevine stilbene synthase multigenic family: genomic organization and expression profiles upon biotic and abiotic stresses, BMC Plant Biol. 12 (2012) 22.
[67] C.C. Celimene, D.R. Smith, R.A. Young, G.R. Stanosz, *In-vitro* inhibition of *Sphaeropsis sapinea* by natural stilbenes, Phytochemistry 56 (2001) 161–165.
[68] R. Pezet, K. Gindro, O. Viret, J.L. Spring, Glycosylation and oxidative dimerization of resveratrol are respectively associated to sensitivity and resistance of grapevine cultivars to downy mildew, Physiol. Mol. Plant Pathol. 65 (2004) 297–303.
[69] N. Stamp, Out of the quagmire of plant defense hypotheses, Q. Rev. Biol. 78 (2003) 23–55.
[70] T. Boller, G. Felix, A renaissance of elicitors: perception of microbe-associated molecular patterns and danger signals by pattern-recognition receptors, Annu. Rev. Plant Biol. 60 (2009) 379–406.
[71] V. Demidchik, ROS-activated ion channels in plants: biophysical characteristics, physiological functions and molecular nature, Int. J. Mol. Sci. 19 (2018) 18.
[72] P. Gong, M. Riemann, D. Dong, N. Stoeffler, B. Gross, A. Markel, P. Nick, Two grapevine metacaspase genes mediate ETI-like cell death in grapevine defence against infection of *Plasmopara viticola*, Protoplasma 256 (2019) 951–969.
[73] B. Kiefer, M. Riemann, C. Büche, H.H. Kassemeyer, P. Nick, The host guides morphogenesis and stomatal targeting in the grapevine pathogen *Plasmopara viticola*, Planta 215 (2002) 387–393.